Superthermal and Efficient-Heating Modes in the Interaction of a Cone Target with Ultraintense Laser Light

H. Nakamura,[1,2] B. Chrisman,[3] T. Tanimoto,[1] M. Borghesi,[4] K. Kondo,[1,2] M. Nakatsutsumi,[1] T. Norimatsu,[2] M. Tampo,[2] K. A. Tanaka,[1,2] T. Yabuuchi,[1] Y. Sentoku,[3] and R. Kodama[1,2,5]

[1]*Graduate School of Engineering, Osaka University, Yamada-oka 2-1, Suita, Osaka, Japan*
[2]*Institute of Laser Engineering, Osaka University, Yamada-oka 2-6, Suita, Osaka, Japan*
[3]*Department of Physics, University of Nevada, Reno, Nevada 89557, USA*
[4]*School of Mathematics and Physics, The Queen's University of Belfast, Belfast BT7 1NN, United Kingdom*
[5]*CREST, Japan Science and Technology Agency, 5-Sanbancho, Chiyoda-ku, Tokyo, Japan*

(Received 6 February 2008; published 30 January 2009)

Interactions between a relativistic-intensity laser pulse and a cone-wire target are studied by changing the focusing point of the pulse. The pulse, when focused on the sidewall of the cone, produced superthermal electrons with an energy >10 MeV, whereas less energetic electrons ~ 1 MeV were produced by the pulse when focused on the cone tip. Efficient heating of the wire was indicated by significant neutron signals observed when the pulse was focused on the tip. Particle-in-cell simulation results show reduced heating of the wire due to energetic electrons produced by specularly reflected light at the sidewall.

DOI: 10.1103/PhysRevLett.102.045009 PACS numbers: 52.50.Jm, 52.38.Kd, 52.40.Mj

Ultraintense lasers produce MeV electron beams at densities of 100 TA/cm^2 [1] when interacting with solid targets. This high energy electron beam quickly heats solid materials and high density plasma to temperatures of order keV. Use of a hollow cone geometry target increases the coupling efficiency of the laser-generated electron beam by a factor of 2–3 over that of a flat geometry target [2].

Interactions between a relativistic-intensity laser ($>10^{18}$ W/cm^2) and a flat foil target at oblique incidence create long-scale electron jets [3,4]. Electrons in these jets are accelerated by the specularly reflected laser light while being collimated by a self-generated magnetic field. In the cone geometry, similar electron jets are created when the laser interacts with the side wall of the cone.

Since the spectrum of electrons generated by a laser hitting a flat target depends upon the obliqueness of incidence, the spectrum of electrons generated by a laser hitting a cone target will also highly depend upon whether the laser predominantly interacts with the side wall of the cone or the flat tip of the cone. The targeting of the laser will determine whether it interacts more with the side wall or more with the tip, providing either an oblique or flat incidence. This effect will greatly influence the energy conversion efficiency from the laser to any material attached to the cone tip.

We studied interactions between a relativistic-intensity laser pulse and a cone-wire target. We observed energetic electron spectra in relativistic laser interactions with a cone target having a wire attached to the tip. We also observed the heating of the wire by energetic electrons when the laser pulse was focused into the cone, while changing the point of irradiation from the tip center (on axis) to the sidewall (off axis) as shown in Fig. 1. Temperatures of the wire were diagnosed by observing spectra of thermal neutrons produced in the deuterated wire. The experimental results show qualitative consistency with two-dimensional collisional particle-in-cell (PIC) simulations with PICLS-2D code [5].

These experiments were carried out using a peta watt laser at Osaka University [6]. The energy was 120 J, the wavelength 1.053 μm, and the pulse duration 0.7–1.1 ps. The pulse was focused by an $f/7.8$ off axis parabola and had a focal spot size of 50 μm, full width at half maximum. A peak intensity of approximately 10^{19} W/cm^2 was obtained at the target. An amplified spontaneous emission pulse started at 4 ns ahead of the main pulse with energy of more than 20 mJ. This amplified spontaneous emission would form a preplasma on the inner wall of the cone.

A deuterated-plastic wire target was attached to the tip of a gold hollow cone. The inner diameter of the tip was approximately 30 μm, its thickness 10 μm and the open-

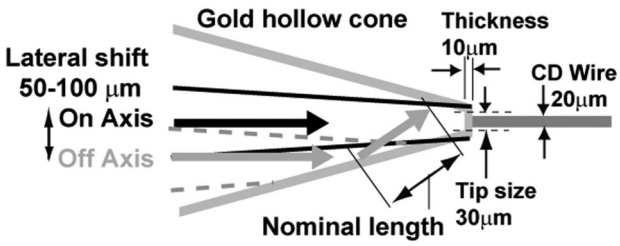

FIG. 1. Experimental configuration. The laser pulse was focused into the cone, while changing the point of irradiation from the tip center (on axis) to the sidewall (off axis). The laser pulse defocused on the side wall. The black solid line represents the focusing angle of the laser pulse in the on axis case and the gray dashed line represents the off axis.

ing angle 30°. The wire diameter was 20 μm. When the laser pulse was focused on the sidewall, the length of the lateral shift perpendicular to the axis of the laser pulse was 50–100 μm and the laser pulse defocused on the side wall, indicating the whole laser pulse interacted with the sidewall outside the tip. The laser pulse was focused with p polarization in the off axis case.

A focusing point of the laser pulse on the cone wall was observed with an x-ray pinhole camera. The x-ray pinhole camera directly observed a time-integrated x-ray image on the inner wall of the cone from the side of laser incidence with smaller angle than the opening angle of the cone.

Electron spectra was observed by an electron spectrometer [7], which was placed along the laser axis. Neutron scintillators were used, which measured the heating temperature of the wire. We observed neutron spectra using a multichannel wave coincidence method to suppress the effects of gamma-ray signals [8].

Figure 2(a) shows the electron energy spectra observed with the electron spectrometer. The black points represent the spectrum in the on axis case while the gray points represent the off axis case. The lower components of the electrons with energies below 1 MeV were an order of magnitude higher in the on axis case in comparison with the off axis case. In the off axis case, higher slope components of temperatures 6–10 MeV appeared on the high energy tail of the spectrum and maximum energy was 50–100 MeV. The maximum energy was 3–4 times higher in the off axis case and the temperature of the on axis case was 2–3 times smaller than that of the off axis case. Taking into account the ponderomotive acceleration [9], the temperature corresponded to that for a laser intensity of about 10^{21} W/cm^2, which is higher by two orders in comparison to actual intensity, indicating that the electrons were additionally accelerated with a different acceleration mechanism. Figure 2(b) shows dependence of the energetic electron temperature on the nominal length. ''Nominal length'' in this context means the length of the electron jet, which corresponds to the distance from the focus point on the side wall to the second point of the reflected light on the tip or on the other side wall as shown in Fig. 1. The typical error bar corresponds to the defocused spot size on the side wall with an oblique incidence.

In the on axis case, significant signals of thermal neutrons were observed. Figure 2(c) shows the spectrum of neutrons generated by a reaction of deuterium-deuterium fusion. The number of the neutrons was about 10^6. In contrasts, when the laser pulse was irradiated on the side wall, thermal neutrons were not observed. The neutron signal for side wall irradiation was less than the detection limit of the diagnostics, in other words less than 10^4. The plasma ion temperature is estimated using the energy spread of thermal neutrons [10]. The observed spectral width of 130 keV corresponded to 1.5 keV for the ion temperature in the on axis case, taking into account the energy resolution of the detector.

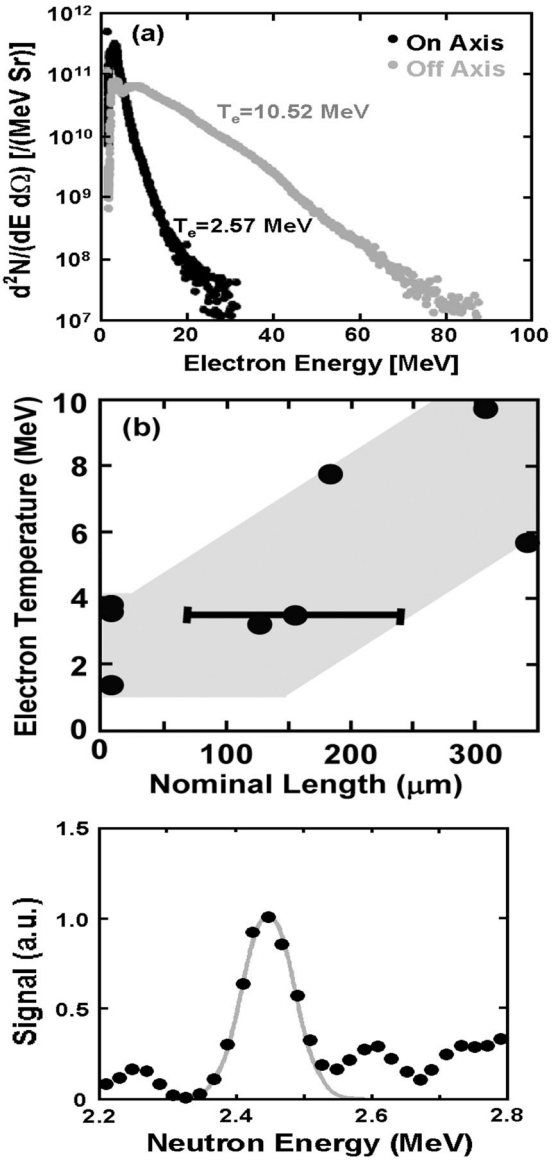

FIG. 2. (a) Electron energy spectra observed with electron spectrometer. The black points represent the spectrum in the on axis case and the gray points in the off axis case. Slope temperatures were 2.57 and 10.52 MeV, respectively. (b) Dependence of the energetic electron slope temperature on the nominal length. (c) Spectrum of neutrons generated by a reaction of deuterium-deuterium fusion. The number of the neutrons was about 10^6.

In order to further understand the discrepancy between the energy conversion efficiencies, we carried out 2 dimensional PIC simulations. Figure 3(a) shows the simulation configuration. The size of the target in the simulations was smaller than that in the experiment while the geometrical configuration was very similar. This reduction was assumed for computational purposes and provides qualitative comparison with the experiment. The tip size of the hollow cone is 8 μm, the thickness of the tip 10 μm, the opening angle of the cone 30°, and the diameter of the wire 4 μm.

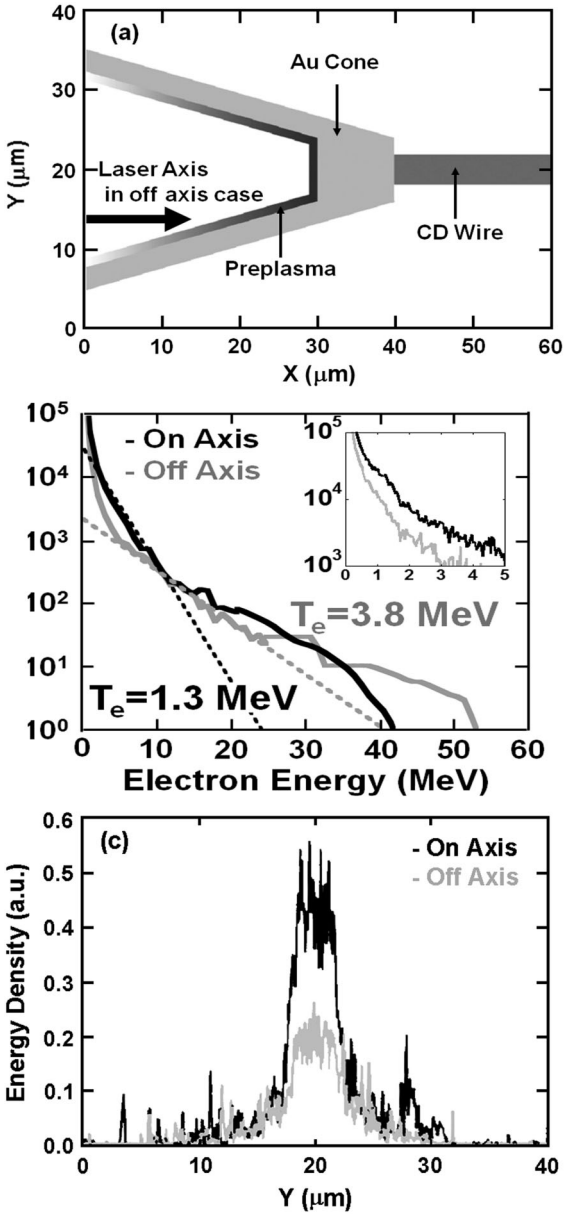

FIG. 3. (a) Simulation configuration. (b) Electron energy spectra calculated at the end of the wire ($X = 50$–60 μm). The inset shows the lower energy population of the energy spectra (below 5 MeV). (c) Deposit energy in the wire target in $X = 50$–60 μm.

The spot size of the laser pulse is 10 μm, and the duration of the representative Gaussian pulse, 500 fs. While the laser intensity does not directly reflect experimental parameters, 10^{20} W/cm^2 was chosen to match the total power input into the cone. The lateral shift-length is 6 μm. The cone density is 1600 n_c and the wire density 160 n_c, respectively, where n_c is the critical density. There is a preplasma layer in front of the cone wall, whose scale length is 0.5 μm. These simulations include binary collisions to simulate the energy deposition in the cone and the plastic wire.

Figure 3(b) shows the electron energy spectra observed by counting electrons at the end of the wire [$X = 50$–60 μm in Fig. 3(a)]. The electron spectrum in the on tip case has a 1.5–2.0 times higher low-energy (below 5 MeV) population than in the off axis case, as shown in the inset of Fig. 3(b) and a lower maximum energy as shown in Fig. 3(b). The slope temperature of the on axis case is 3 times smaller than that of the off axis case. Figure 3(c) shows the deposited energy in the wire target. These results indicate 2 times more energy is deposited inside the wire in the on axis case than in the off axis case. The results qualitatively demonstrate the differing acceleration mechanisms due to sidewall and cone-tip interactions and their impact upon heating the attached wire.

Figures 4(a) and 4(b) show the magnetic field distribution in the on axis and off axis cases, respectively. The magnetic field around the wire is higher in the on axis case when compared with that in the off axis case, indicating the higher energy density electrons propagate in the wire in the on axis case.

Figures 4(c) and 4(d) show the electron energy density distribution in on axis and off axis cases, respectively. In Fig. 4(d), the solid lines represent the laser incidence axis and the specular direction, and the dotted lines indicate the initial cone position. Electron jets are observed in the specular direction as shown in Fig. 4(d). In previous experiments of oblique incidence on a foil target, jetlike x-ray emission in the specular direction was also observed and simulations show the specularly reflected laser light is temporally modulated near the critical point in a plasma consisting of a steep density gradient [3]. At the sidewall of the cone, similar phenomena were also expected to be generated. The modulation can be explained by absorption at the reflection point, the stimulated Raman scattering [11]. The modulated laser light excites plasma waves. The energetic electrons are accelerated in the plasma waves by laser wakefield acceleration. Therefore, in the off axis case, energetic electrons accelerations were enhanced by the specularly reflected laser light. While in the on axis case, interface steepening occurs at the tip of the cone due to strong photon pressure of the focused light. As a result, a large number of less energetic ($\sim$ MeV) electrons are produced as discussed in Ref. [12]. These MeV electrons heat the wire effectively as seen in Fig. 3(c). On the other hand, without the preplasma on the inner wall of the cone, the electron jets might not have been produced as discussed in Ref. [4] and the electron temperature might not have increased in the off axis case. Therefore, the electron temperature is sensitive to the parameters of the preplasma.

In conclusion, we have measured energetic electron spectra in the relativistic intense laser interaction with a cone-wire target. We also measured the fast heating of the wire by the electrons when the laser pulse was focused into the cone, while changing the point of interaction from the tip center to the side wall. Higher slope components ap-

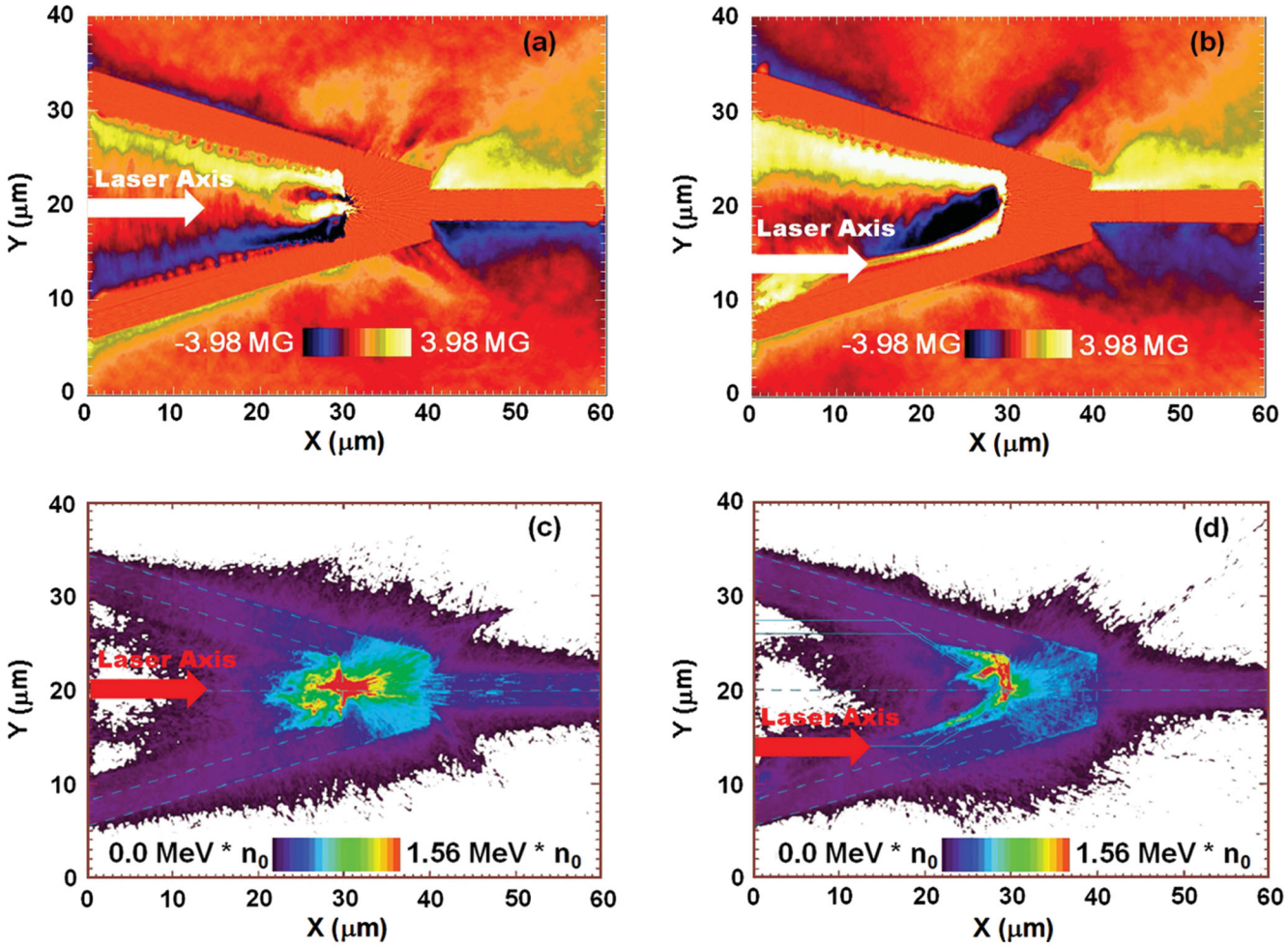

FIG. 4 (color). Magnetic field distributions in the on axis case (a) and in the off axis case (b) at $t = 500$ fs. Electron energy density distributions in the on axis case (c) and in the off axis case (d) at $t = 500$ fs. Dotted lines in (c) and (d) represent initial cone positions. Blue solid lines show the laser axis and specular directions of the laser pulse.

peared in the high energy tail of the electron energy spectra in the off axis case. In contrast, when the laser interacted directly with the tip of the cone, the lower energy electron component increased on the wire, resulting in relatively efficient heating of the wire to more than 1 keV. PIC simulations show the electrons are accelerated to energies above 60 MeV by a modulated laser pulse in the sidewall interaction. Therefore, changing the focusing points on the cone wall creates two different modes of heating and accelerations, each of which can be used for different potential applications.

We acknowledge all the technical support provided by the engineering staffs at the Institute of Laser Engineering. This work is partially supported by a grant for the Osaka University Global COE Program, CEDI, from the Ministry of Education, Culture, Sports, Science and Technology of Japan. B. C. is supported by U.S. Department of Energy under Cooperative Agreement DE-FC02-04ER54789.

[1] K. B. Wharton *et al.*, Phys. Rev. Lett. **81**, 822 (1998); R. Kodama *et al.*, Phys. Plasmas **8**, 2268 (2001).
[2] R. Kodama *et al.*, Nucl. Fusion **44**, S276 (2004); Y. Sentoku *et al.*, Phys. Plasmas **11**, 3083 (2004).
[3] R. Kodama *et al.*, Phys. Rev. Lett. **84**, 674 (2000).
[4] Y. Sentoku *et al.*, Phys. Plasmas **6**, 2855 (1999).
[5] Y. Sentoku and A. J. Kemp, J. Comput. Phys. **227**, 6846 (2008).
[6] Y. Kitagawa *et al.*, IEEE J. Quantum Electron. **40**, 281 (2004).
[7] K. A. Tanaka *et al.*, Rev. Sci. Instrum. **76**, 013507 (2005).
[8] H. Nakamura *et al.*, Rev. Sci. Instrum. **77**, 10E727 (2006).
[9] S. C. Wilks, W. L. Kruer, M. Tabak, and A. B. Langdon, Phys. Rev. Lett. **69**, 1383 (1992).
[10] H. Brysk, Plasma Phys. **15**, 611 (1973).
[11] S. V. Bulanov *et al.*, Phys. Plasmas **1**, 745 (1994).
[12] B. Chrisman *et al.*, Phys. Plasmas **15**, 056309 (2008).